

Improvement on Sensorless Vector Control Performance of PMSM with Sliding Mode Observer

Wahyu Kunto Wibowo*, Seok-Kwon Jeong*† and Young-Mi Jung***

(Received 13 June, Revised 16 September, Accepted 16 September)

Abstract: This paper proposes improvement on sensorless vector control performance of a permanent magnet synchronous motor (PMSM) with sliding mode observer. An adaptive observer gain and second order cascade low-pass filter (LPF) were used to improve the estimation accuracy of the rotor position and speed. The adaptive observer gain was applied to suppress the chattering intensity and obtained by using the Lyapunov's stability criterion. The second order cascade LPF was designed for the system to escalate the filtering performance of the back-emf estimation. Furthermore, genetic algorithm was used to optimize the system PI controller's performance. Simulation results showed the effectiveness of the suggested improvement strategy. Moreover, the strategy was useful for the sensorless vector control of PMSM to operate on the low-speed area.

Key Words : Permanent Magnet Synchronous Motor, Sensorless Vector Control, Adaptive Observer Gain, Second Order Cascade Low Pass Filter, Sliding Mode Observer, Genetic Algorithm, Robustness.

1. Introduction

Due to the benefits such as high power density, high speed and high efficiency, permanent magnet synchronous motor (PMSM) is widely used not only in industrial field, but also in home appliances and research field. The control technique known as vector control has been used to obtain high performance control on PMSM.^{1,2)} However,

conventional vector control needs a sensor for detecting speed and rotor flux position to ensure the control precision. The existence of the sensor presents some disadvantages such as drive cost, installation, reliability and noise immunity.

The sensorless algorithm has been receiving high attention from many researchers to overcome disadvantages of the sensed system. There are two kinds of representative sensorless algorithm which preferred for the PMSM system: signal injection method and state observer method. State observer method which also known as model based approach, is preferably to use in sensorless applications. The state observer method which includes Kalman filter, model reference adaptive system, and sliding mode observer (SMO) are preferred for medium to high speed operation. These methods estimate the back-emf or the flux linkage to calculate the current

*† Seok-Kwon Jeong(corresponding author) : Department of Refrigeration and Air-Conditioning, Pukyong National University.

E-mail : skjeong@pknu.ac.kr, Tel : 051-629-6181

*Wahyu Kunto Wibowo : Department of Interdisciplinary Program of Mechatronics Engineering, Pukyong National University.

***Young-Mi Jung : Department of Refrigeration and Air-Conditioning, Pukyong National University.

rotor position.³⁻⁵⁾ Many researchers are interested in SMO because of its advantages such as robustness against system parameter variations compared to other types of state observer methods.

In conventional SMO, signum function is used to estimate the back-emf of the PMSM. Low pass filter (LPF) is taking a place in this method to refine the switching signal result and reduce the chattering problem caused by signum function. Jung et al did the simulations and experiments and the results show that the estimated position tracks the actual position by using the signum function.⁶⁾ Lee et al used sigmoid function as signum function replacement in SMO for PMSM sensorless control. The chattering problems were successfully reduced by using the sigmoid function.⁷⁾

In this paper, adaptive observer gain and second order cascade LPF are proposed to decrease the chattering problem caused by the switching function. The adaptive gain is easily obtained from the speed command and motor flux linkage parameter according to Lyapunov's stability analysis derivation. The second order cascade LPF is used as the filtering method to decrease the chattering problems and to obtain smooth back-emf estimation. Moreover, genetic algorithm (GA) is used on PI controllers gain design to improve the system control performance. Finally, the performance and effectiveness of the proposed method are verified from simulation results.

2. Mathematical model of PMSM

Mathematical model of PMSM in α, β stationary reference frame is shown in Eq. (1).

$$\begin{bmatrix} v_\alpha \\ v_\beta \end{bmatrix} = \begin{bmatrix} R_s + pL_s & 0 \\ 0 & R_s + pL_s \end{bmatrix} \begin{bmatrix} i_\alpha \\ i_\beta \end{bmatrix} + \begin{bmatrix} e_\alpha \\ e_\beta \end{bmatrix} \quad (1)$$

$$\begin{bmatrix} e_\alpha \\ e_\beta \end{bmatrix} = \omega_r \psi_r \begin{bmatrix} -\sin\theta_r \\ \cos\theta_r \end{bmatrix} \quad (2)$$

Where $v_\alpha, v_\beta, i_\alpha,$ and i_β are the stator voltages and currents in stationary reference frame. R_s and L_s are the stator resistance and inductance. ω_r and ψ_r represent rotor angular speed and flux linkage generated by the rotor magnet. Notation p is the derivative of time. Also, e_α and e_β are back-emf in α, β stationary reference frame. Symbol θ_r represents position of the rotor flux. Eq. (1) is used to design the current observer. It is noted that all the motor parameters are assumed as constant value which makes the observer design much easier.

3. Observer and controller design

3.1 Sliding mode observer

A typical structure of sensorless vector control of PMSM with sliding mode observer is shown in Fig. 1. The SMO is utilized in the system as a replacement of the physical sensor for obtaining rotor flux position and speed information. At first, the back-emf is estimated from current and supply voltage of the motor, then the result is used to estimate the position and speed at SMO. The estimated position and speed are given as the feedback information for the vector control algorithm.

Eq. (1) is rearranged to design the sliding mode observer as follow:

$$\begin{bmatrix} p i_\alpha \\ p i_\beta \end{bmatrix} = -\frac{R_s}{L_s} \begin{bmatrix} i_\alpha \\ i_\beta \end{bmatrix} + \frac{1}{L_s} \begin{bmatrix} v_\alpha \\ v_\beta \end{bmatrix} - \frac{1}{L_s} \begin{bmatrix} e_\alpha \\ e_\beta \end{bmatrix} \quad (3)$$

The sliding surface is selected as:

$$S = \hat{i}_s - i_s \quad (4)$$

where $i_s = [i_\alpha \ i_\beta]^T$ is the actual value and $\hat{i}_s = [\hat{i}_\alpha \ \hat{i}_\beta]^T$ is the estimated value. The SMO in Eq. (5) can be designed directly from Eq. (3):

$$\begin{bmatrix} p\hat{i}_\alpha \\ p\hat{i}_\beta \end{bmatrix} = -\frac{R_s}{L_s} \begin{bmatrix} \hat{i}_\alpha \\ \hat{i}_\beta \end{bmatrix} + \frac{1}{L_s} \begin{bmatrix} v_\alpha \\ v_\beta \end{bmatrix} - \frac{1}{L_s} \begin{bmatrix} z_\alpha \\ z_\beta \end{bmatrix} \quad (5)$$

$$\begin{bmatrix} z_\alpha \\ z_\beta \end{bmatrix} = K \begin{bmatrix} \text{sign}(\hat{i}_\alpha - i_\alpha) \\ \text{sign}(\hat{i}_\beta - i_\beta) \end{bmatrix} \quad (6)$$

where the symbol hat “ \wedge ” denotes the estimated value and K is observer gain. Symbol z is the switching signal which contains the estimated back-emf information. $\text{sign}(x)$ is the signum function and it is represented as:

$$\text{sign}(x) = \begin{cases} 1, & x > 0 \\ 0, & x = 0 \\ -1, & x < 0 \end{cases} \quad (7)$$

The dynamic estimation error can be obtained by subtracting Eq. (3) from Eq. (5):

$$\begin{bmatrix} p\bar{i}_\alpha \\ p\bar{i}_\beta \end{bmatrix} = -\frac{R_s}{L_s} \begin{bmatrix} \bar{i}_\alpha \\ \bar{i}_\beta \end{bmatrix} + \frac{1}{L_s} \begin{bmatrix} e_\alpha \\ e_\beta \end{bmatrix} - \frac{1}{L_s} \begin{bmatrix} z_\alpha \\ z_\beta \end{bmatrix} \quad (8)$$

where the symbol bar represents estimation error of the corresponding variable. When the estimated current reaches the sliding surface ($s=0$), then the estimation error becomes zero and the estimated current tracks the actual value. Hence, $\hat{i}_s = i_s$, Eq. (8) will give:

$$e_s = [e_\alpha \ e_\beta]^T = K \text{sign}(\bar{i}_s) \quad (9)$$

Signum function is used in SMO to generate the estimated back-emf. However, this function induces the chattering problems. First order LPF is taking a place in the algorithm to overcome this problem, as shown in Eq. (10).

$$[\hat{e}_\alpha \ \hat{e}_\beta]^T = \frac{\omega_c}{s + \omega_c} [z_\alpha \ z_\beta]^T \quad (10)$$

Where ω_c is the cut-off frequency of the LPF. The estimated back-emf results are directly used to calculate the rotor flux position as follows:

$$\hat{\theta}_r = -\tan^{-1} \frac{\hat{e}_\alpha}{\hat{e}_\beta} \quad (11)$$

Furthermore, the estimated back-emfs are used to calculate the speed according to Eq. (2) as follows:

$$|\hat{\omega}_r| = \frac{1}{\psi_r} \sqrt{\hat{e}_\alpha^2 + \hat{e}_\beta^2} \quad (12)$$

Fig. 2 shows the structure of the conventional SMO on the PMSM sensorless control system.

3.2 Design of an adaptive observer gain

The SMO is also known as high gain observer

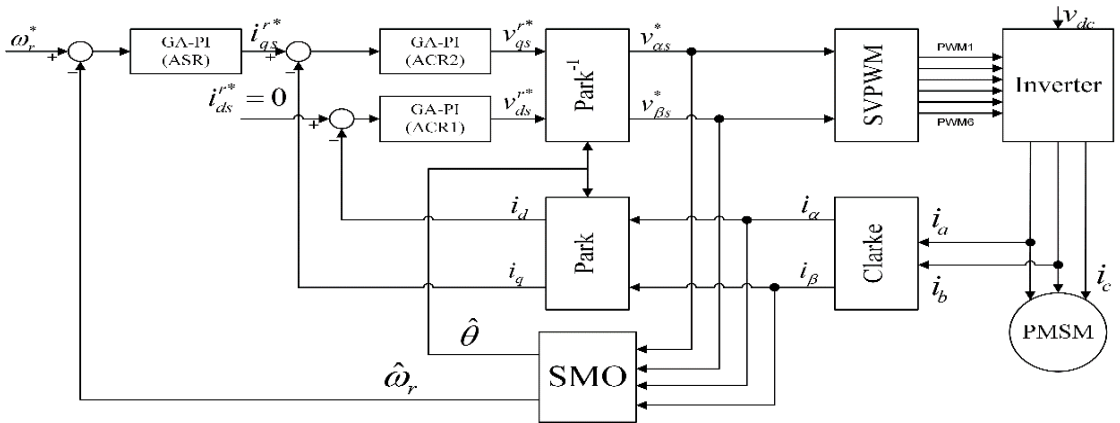


Fig. 1 Block diagram of PMSM sensorless control with SMO

which has appropriate behavior in disturbance rejection.⁸⁾ The noise and chattering problems are magnified because of the high gain usage. However, the estimation results will be deteriorated if the gain is too small. Hence, appropriate gain is desirable to suppress the chattering problems. An adaptive observer gain is designed to overcome the problem.

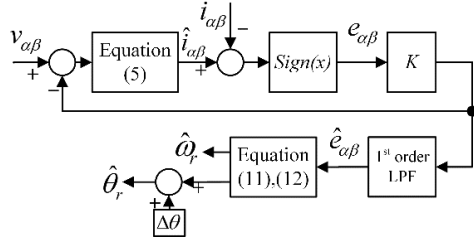


Fig. 2 Structure of conventional SMO

The sliding surface is defined as the estimation error of the stator current, which is shown in Eq. (4). When the condition $\dot{S}S < 0$ is satisfied, the sliding mode exist, and this implies that $S \rightarrow 0$ for $t \rightarrow \infty$, $S_\alpha = \bar{i}_\alpha$, and $S_\beta = \bar{i}_\beta$. Lyapunov function candidate is defined in Eq. (13) to design the adaptive observer gain and to set up the stability condition of the SMO.

$$V = \frac{1}{2} S^T S = \frac{1}{2} \bar{i}_\alpha^2 + \bar{i}_\beta^2 \quad (13)$$

Since V is positive definite ($V > 0$), the equilibrium point $V = 0$ is asymptotically stable when \dot{V} is negative definite ($\dot{V} < 0$), hence:

$$\dot{V} = p \bar{i}_\alpha \dot{\bar{i}}_\alpha + p \bar{i}_\beta \dot{\bar{i}}_\beta \quad (14)$$

Eq. (15) is obtained by substituting Eq. (8) into Eq. (14).

$$\begin{aligned} \dot{V} = & -\frac{R_s \bar{i}_\alpha^2}{L_s} + \frac{\bar{i}_\alpha e_\alpha}{L_s} - \frac{\bar{i}_\alpha}{L_s} K \text{sign}(\bar{i}_\alpha) \\ & -\frac{R_s \bar{i}_\beta^2}{L_s} + \frac{\bar{i}_\beta e_\beta}{L_s} - \frac{\bar{i}_\beta}{L_s} K \text{sign}(\bar{i}_\beta) \end{aligned} \quad (15)$$

Then, Lyapunov function is satisfied when:

$$K > \max(|e_\alpha|, |e_\beta|) \quad (16)$$

Eq. (2) shows the back-emf formula. The back-emf will reach the maximum when the values of $\sin \theta_r$ and $\cos \theta_r$ are equal to 1. Hence, the adaptive observer gain of Eq. (17) can be obtained substituting Eq. (2) to Eq. (16).

$$K = \omega_r^* \psi_r \quad (17)$$

Where ω_r^* is reference speed. With this adaptive method, the observer is enough to estimate the back-emf precisely and able to suppress the chattering problems.

3.3 Design of second order cascade LPF

In the conventional SMO system, first order LPF was used to eliminate the chattering problem caused by the switching function and high gain of the observer. However, the attenuation performance of this filter somehow not enough to suppress the chattering phenomena. Second order cascade LPF is proposed in this paper to replace the first order LPF. The second order cascade LPF, Eq. (18), attenuates twice as fast as the first order LPF.

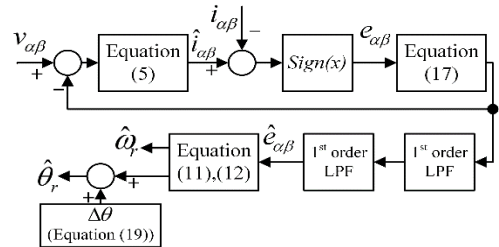


Fig. 3 Structure of the proposed SMO

$$LPF_{2nd} = \frac{\omega_c^2}{s^2 + 2\omega_c s + \omega_c^2} \quad (18)$$

However, the usage of this filter causes a long time delay in estimating the position of the rotor. Furthermore, the time delay of the position is caused by the variation of the estimated rotor speed. The phase delay $\Delta\theta$ compensation is needed to overcome the delay, and it is calculated as follows:

$$\Delta\theta = \tan^{-1} \frac{2\hat{\omega}_r}{\omega_c - \hat{\omega}_r^2} \quad (19)$$

Fig. 3 shows the structure of the proposed SMO.

The PI controllers of sensorless PMSM control shown in Fig. 1 including proposed SMO is optimized by using GA method to improve the system control performance.^{9,10)}

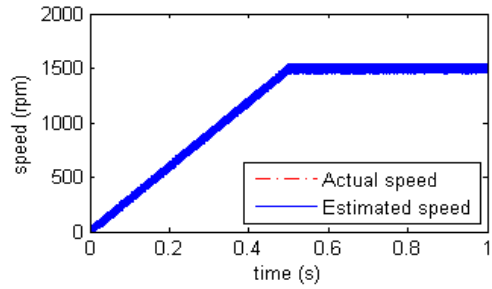
Table 1 Parameters of PMSM

Parameter (symbol)	Value (unit)
Rated power	2.2 (kW)
Rated torque	7 (N.m)
Rated speed	3000 (rpm)
Stator resistance (R_s)	0.141 (Ω)
Stator inductance (L_s)	$1.755e^{-3}$ (H)
Flux linkage (ψ_r)	0.1054 (Wb)
Inertia	$10.4e^{-4}$ (Kg.m)
Friction coefficient	$1e^{-4}$ (N.m.s/rad)
Pole number	8

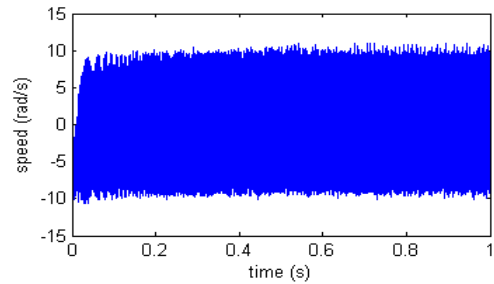
4. Simulation results and analysis

System in Fig. 1 has been simulated in the Matlab/Simulink environment in order to verify the validity of the proposed system. Table 1 shows the parameters of the PMSM.

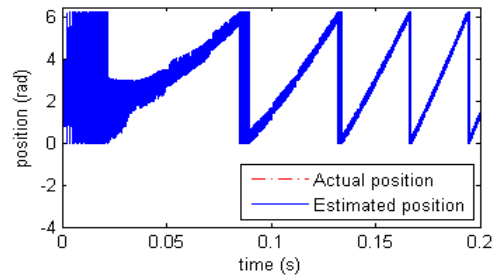
Fig. 4 shows the simulation result of the PMSM sensorless vector control with conventional SMO. A constant observer gain and first order LPF are used on the conventional SMO. The constant gain observer K was set as 150 and the cut-off frequency ω_c of the LPF was set as 1500 Hz. It can be seen



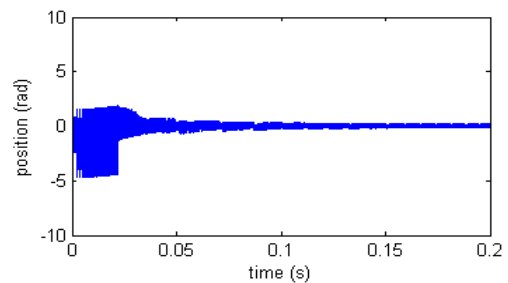
(a) Speed responses



(b) Speed estimation error



(c) Rotor flux position estimation



(d) Rotor flux position estimation error

Fig. 4 Sensorless control results with conventional SMO

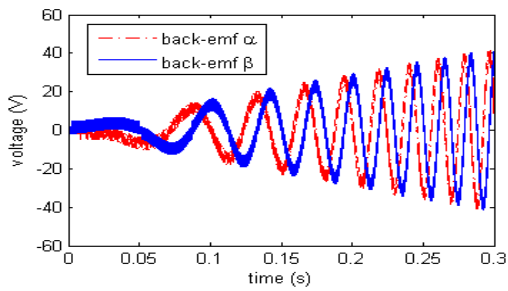
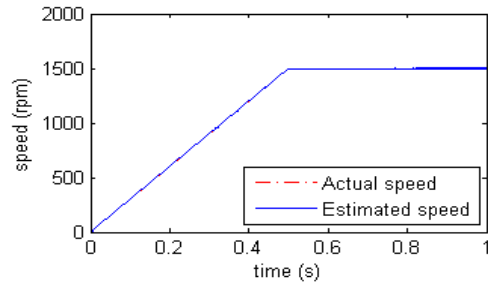


Fig. 5 Chattering problems of back-emf α and β with conventional SMO

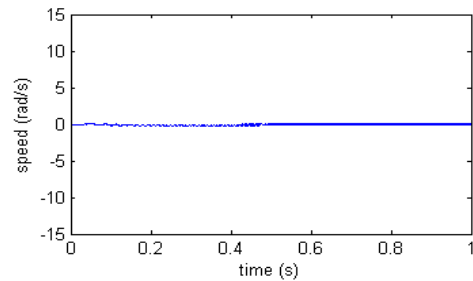
that the chattering was big and disturbed the estimation accuracy of speed and position especially during transient time. This is because of the observer gain was too big and the chattering was enlarged by this high gain during transient time. Appropriate observer gain K is needed to decrease the chattering magnification caused by the high observer gain. The adaptive observer gain K is used to overcome that problem.

Fig. 5 shows the chattering problems of back-emfs on a system which used conventional SMO. The chattering which occurred on the back-emf estimation results shown in Fig. 5, included harmonic disturbances and the amplitude of the harmonics is considerably high. Based on this, the second order cascade LPF is proposed to suppress the chattering problems.

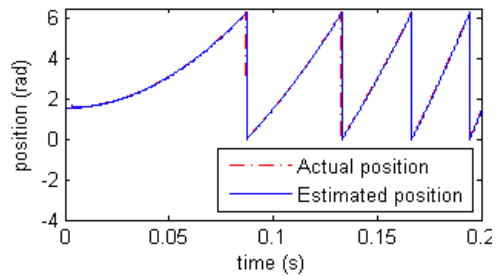
Fig. 6 shows simulation results of PMSM sensorless control with the proposed SMO system. The proposed SMO was applying the adaptive observer gain and second order cascade LPF. From Fig. 6, it can be seen that the estimation accuracy was improved compared to the conventional SMO result. This results were acquired because of decrement on the back-emf estimation error. The chattering problems which happened during transient time were suppressed efficiently by using appropriate adaptive observer gain K . Furthermore, the chattering caused by the signum function was



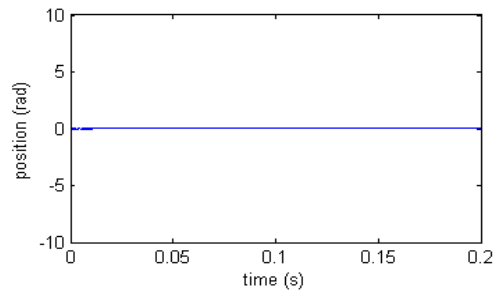
(a) Speed responses



(b) Speed estimation error



(c) Rotor flux position estimation



(d) Rotor flux estimation error

Fig. 6 Sensorless control results with the proposed SMO

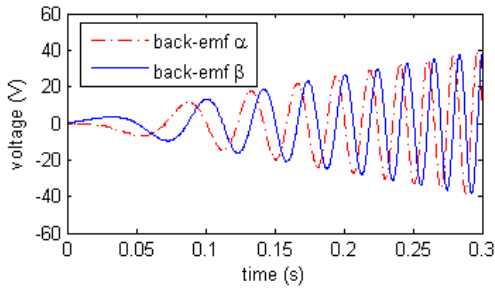


Fig. 7 Back-emf α and β with the proposed SMO

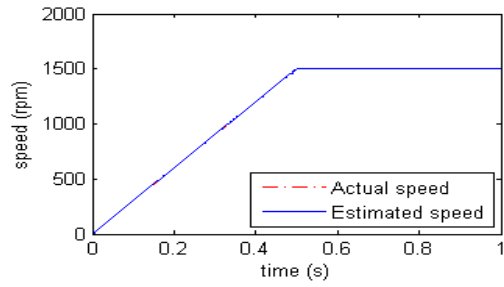
successfully decreased by the second order cascade LPF.

Fig. 7 shows the back-emfs on the proposed SMO. From Fig. 7, it can be seen that the chattering was successfully decreased by the proposed strategy. This significant improvement shows that the proposed SMO method was desirable as the observer on the PMSM sensorless control to reach high precision control performance. Table 2 shows the comparison of the performance between conventional SMO and the proposed SMO.

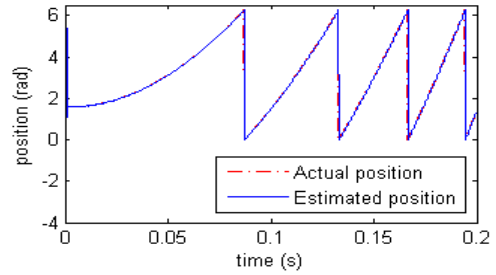
Fig. 8 shows the results when two parameters of the system shown in Table 1 were changed purposely to verify the robustness of the system. \tilde{R}_s and \tilde{L}_s denotes 20% decrement from the nominal value of the two parameters. From Fig. 8, it shows that even though some parameters were changed from real values, the system can still give good responses. This implies that the proposed system has strong robustness. Fig. 9 shows the speed response in low-speed region. The result confirms that the estimated speed was able to track the actual speed

Table 2 Comparison of performance between conventional SMO and the proposed SMO

SMO Method	Chattering	Speed error accuracy
Conventional	40%	10 rad/s
Proposed	18%	0.3 rad/s
Improvement	55%	97%



(a) Speed responses



(b) Rotor flux position estimation

Fig. 8 Proposed sensorless control results with parameter variation

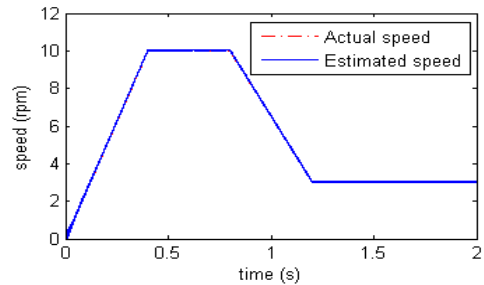


Fig. 9 Speed response in low-speed region by the proposed SMO

in low-speed region accurately. This means that the back-emf was precisely estimated by the proposed system in low-speed area. Based on the Eq. (11) and (12), if the chattering problems occurred on the back-emf estimation can be suppressed as minimum as possible, then the precision of the speed and position estimation will increase. Hence, it will contribute to achieve good sensorless operation of PMSM in very low-speed.

5. Conclusions

This paper proposed an improvement on sensorless vector control performance of PMSM with SMO. Based on the simulation results, the adaptive observer gain managed to decrease the chattering problems caused by the high constant observer gain especially during the transient time. In other hand, the second order cascade LPF succeeded to lessen the chattering problems on the estimation results in the steady-state time effectively. The proposed strategy combining those two methods succeeded to reduce the chattering significantly whether at transient state and steady-state. Furthermore, the speed estimation in low-speed area was giving a good tracking performance. This is because of the deterioration on the back-emf estimation caused by the chattering problems can be overcome by applying the suggested strategy. Moreover, optimization of PI controllers by the GA increased the control performance and robustness of the PMSM sensorless control system.

References

1. L. Zhong, M. F. Rahman, W. Y. Hu, and K. W. Lim, 1997, "Analysis of Direct Torque Control in Permanent Magnet Synchronous Motor Drives," *IEEE Trans. Power Electr.* Vol. 12, No. 3, pp. 528-536.
2. B. Shikkewal and V. Nandanwar, 2012, "Fuzzy Logic Controller for PMSM," *Int. J. Electr. Electron. Eng.*, Vol. 1, No. 3, pp. 73-78.
3. L. Baohua, Y. Jianhua, and L. Weiguo, 2009, "Study on speed sensorless SVM-DTC system of PMSM," *9th Int. Conf. Electron. Meas. Instruments*, pp. 2.914-2.919.
4. Y. S. Kung and N. T. Hieu, 2013, "Simulink / Modelsim Co-Simulation of EKF-based Sensorless PMSM Drives," *10th Int. Conf. Power Electron. Drive Syst.(PEDS)*, 2013 IEEE, pp. 709-713.
5. N. Öztürk and E. Çelik, 2012, "Speed control of permanent magnet synchronous motors using fuzzy controller based on genetic algorithms," *Int. J. Electr. Power Energy Syst.*, Vol. 43, No. 1, pp. 889-898.
6. Y. S. Jung and M. G. Kim, 2009, "Sliding Mode Observer for Sensorless Control of IPMSM Drives," *J. of Power Electronics*, Vol. 9, No. 1, pp. 117-123.
7. H. Lee and J. M. Lee, 2013, "Design of Iterative Sliding Mode Observer for Sensorless PMSM Control," *IEEE Trans. Control Syst. Technol.*, Vol. 21, No. 4, pp. 1394-1399.
8. M. Hajatipour and M. Farrokhi, 2010, "Chattering free with noise reduction in sliding-mode observers using frequency domain analysis," *J. Process Control*, Vol. 20, No. 8, pp. 912-921.
9. S. K. Jeong and W. K. Wibowo, 2013, "Optimization of PI Controller Gain for Simplified Vector Control on," *Journal of Korean Society for Power System Engineering*, Vol. 17, No. 5, pp. 90-97.
10. W. K. Wibowo and S. K. Jeong, 2013, "Genetic algorithm tuned PI controller on PMSM simplified vector control," *J. Cent. South Univ.*, Vol. 20, No. 11, pp. 3042-3048.
11. W. K. Wibowo, S. K. Jeong, and Y. M. Jung, 2014, "Chattering Reduction of Sliding Mode Observer on Sensorless Vector Control of PMSM," *Proc. of Korean Society for Power System Engineering*, pp. 164-165.